ISSN 0915-633X

NATIONAL INSTITUTE FOR FUSION SCIENCE

Electron Collision Effects on the Bremsstrahlung Emission in Lorentzian Plasmas

Young-Dae Jung and D. Kato

(Received - May 28, 2009)

NIFS-952

June 30, 2009

RESEARCH REPORT
NIFS Series

TOKI, JAPAN

Electron collision effects on the bremsstrahlung emission in Lorentzian plasmas

Young-Dae Jung[1,2] and Daiji Kato[1]

[1]National Institute for Fusion Science, Toki, Gifu, 509-5292, Japan
[2]Department of Applied Physics, Hanyang University, Ansan, Kyunggi-Do 426-791, South Korea

E-mail: ydjung@hanyang.ac.kr

Abstract

The electron-electron collision effects on the electron-ion bemsstranhlung process are investigated in warm Lorentzian plasmas. The effective electron-ion interaction potential is obtained by including the far-field terms caused by the electron-electron collisions with the effective Debye length in Lorentzian plasmas. The bremsstranhlung radiation cross section is obtained as a function of the electron energy, photon energy, collision frequency, spectral index, and Debye length using the Born approximation for the initial and final states of the projectile electron. It is shown that the non-Maxwellian character suppresses the bremsstrahlung radiation cross section. It is also shown that the electron-electron collision effect enhances the bremsstrahlung emission spectrum. In addition, the bremsstrahlung radiation cross section decreases with an increase of the plasma temperature.

Keywords: electron-ion bremsstrahlung radiation, Lorentzian plasma

PACS number: 52.20.-j

The electron-ion bremsstrahlung processes [1-7] have received much attention since these processes have been widely used in plasma diagnostics in various astrophysical and laboratory weakly coupled plasmas. Many of the characteristic properties of plasmas would be understood by knowing the velocity dependence of the distribution function of plasma particles. It is shown that the isotropic Maxwellian plasma is in thermal equilibrium which implies that it no longer contains free energy and, hence, there are no energy exchanges between plasma particles. However, in numerous cases of astrophysical and laboratory plasmas, the coupling of the external field with the equilibrium plasma often generates superthermal electrons departed from the conventional Maxwellian velocity distribution [8-10]. Moreover, it has been shown that the far-field potential terms of a test charge apart from the ordinary Debye-Hückel screening term has to be included in order to properly describe the particle interactions in collisional plasmas [11,12]. Hence, the electron-ion bremsstrahlung process in collisional non-Maxwellian plasmas would be quite different from those in collisionless Maxwellian plasmas due to the influence of the non-Mxwellian character and electron-electron collision effects. Thus, in this paper we investigate the physical properties of the electron-ion bremsstrahlung process in warm collisional Lorentzian plasmas. The effective screened potential model [12] including the additional far-field potential due to electron-electron collisions apart from the ordinary Debye-Hückel shielding term with the effective Debye length is employed to describe the appropriate screened electron-ion interactions in collisional Lorentzian plasmas. The nonrelativistic Born approximation [1] is employed for both the initial and final states of the projectile electron to obtain the electron-ion bremsstrahlung radiation cross section including the electron-electron collision and non-Maxwellian effects..

Using the second-order nonrelativistic perturbation analysis [3], the differential electron-ion bremsstrahlung cross section $d^2\sigma_b$ can be written as

$$d^2\sigma_b = d\sigma_C \cdot dW_\omega , \tag{1}$$

where $d\sigma_C$ is the differential elastic scattering cross section:

$$d\sigma_C = \frac{1}{2\pi\hbar v_0^2}\left|\tilde{V}(\mathbf{q})\right|^2 q\, dq, \tag{2}$$

v_0 is the initial velocity of the projectile electron, $\tilde{V}(\mathbf{q})$ is the Fourier transformation of the electron-ion interaction potential $V(\mathbf{r})$:

$$\tilde{V}(\mathbf{q}) = \int d^3\mathbf{r}\, e^{-i\mathbf{q}\cdot\mathbf{r}}\, V(\mathbf{r}), \tag{3}$$

$\mathbf{q}(=\mathbf{k}_0 - \mathbf{k}_f)$ is the momentum transfer, and $\mathbf{k}_0$ and $\mathbf{k}_f$ are the wave vectors of the initial and final states of the projectile electron, respectively. Here, dW_ω is the differential probability of emitting a photon of frequency between ω and $\omega + d\omega$ in the solid angle $d\Omega$:

$$dW_\omega = \frac{\alpha}{4\pi^2}\Lambda^2 \sum_{\hat{\mathbf{e}}}\left|\hat{\mathbf{e}}\cdot\mathbf{q}\right|^2 \frac{d\omega}{\omega} d\Omega, \tag{4}$$

where $\alpha(=e^2/\hbar c \cong 1/137)$ is the fine structure constant, $\Lambda(=\hbar/mc)$ is the Compton wave number, m is the electron mass, and $\hat{\mathbf{e}}$ is the unit photon polarization vector. By integrating over the directions of the radiation photon, we then obtain the following form of the bremsstrahlung cross section:

$$d^2\sigma_b = \frac{1}{3\pi^2\beta_0^2}\frac{\alpha}{(mc^2)^2}\left|\tilde{V}(\mathbf{q})\right|^2 q^3\, dq \frac{d\omega}{\omega}, \tag{5}$$

since the summation over polarizations gives the angular distribution factor $\sin^2\theta$, where θ is the angle between $\mathbf{k}_0$ and $\mathbf{q}$, and $\beta_0 = v_0/c$.

In various astrophysical and laboratory plasmas, the important departures from the equilibrium Maxwellian distribution function would be expected due to the strong external disturbances. These so-called superthermal electrons escape the ordinary

Maxwellian distribution corresponding to the bulk of plasma electrons, which can be illustrated more effectively by the Lorentzian velocity distribution [8,10]. Moreover, an exquisite work by Hasegawa, *et al.* [8] has proved that the equilibrium plasma distribution function in the presence of the superthermal radiation field resembles the Lorentzian distribution function. In Lorentzian plasmas [10], the characteristic energy E_κ is expressed by $E_\kappa = [(\kappa - 3/2)/\kappa]E_T$, where κ is the spectral index, $E_T \equiv k_B T$, k_B is the Boltzmann constant, and T is the plasma temperature. It is also shown that the effective Debye radius λ_κ in Lorentzian plasmas [10] can be represented by $\lambda_\kappa \equiv \eta_\kappa \lambda_D$, where $\eta_\kappa \equiv [(\kappa - 3/2)/(\kappa - 1/2)]^{1/2}$ and λ_D is the conventional Debye length in Maxwellian plasmas. In addition, the effective screened potential [12] of a moving test charge in warm collisional plasmas has been obtained by the Poisson equation and linearized collision operator C_L in the full BGK model [13] with the plasma dielectric function including the effects of electron-electron collisions. Using the effective potential model [12], we then obtain the screened interaction potential $V_{e-Ze}(\mathbf{r})$ between the electron and ion with nuclear charge Ze including the influence of electron-electron collisions in warm collisional Lorentzian plasmas when $v_0 < v_\kappa$:

$$V_{e-Ze}(\mathbf{r}) = -\frac{Ze^2}{r} e^{-r/\lambda_\kappa} - Ze^2 \frac{4}{\sqrt{2\pi}} \frac{\cos\gamma}{r} \left(\frac{\lambda_\kappa}{r}\right)^2 \left(\frac{v_0}{v_\kappa}\right) \left[1 + \frac{\sqrt{2\pi}}{4}\left(2 - \frac{7\pi}{12}\right)\frac{\nu r}{v_\kappa}\right], \quad (6)$$

where γ is the angle between $\mathbf{v}_0$ and $\mathbf{r}$, $v_\kappa \equiv \mu_\kappa v_T$, $\mu_\kappa \equiv [(\kappa - 3/2)/\kappa]^{1/2}$, $v_T = \lambda_D \omega_p$, ω_p is the plasma frequency, and ν is the electron-electron collision frequency. As shown, the effective interaction potential $V_{e-Ze}(\mathbf{r})$ comprises the additional terms due to electron-electron collisions apart from the ordinary Debye-Hückel screening potential $(-Ze^2/r)e^{-r/\lambda_\kappa}$. After some mathematical manipulations in the cylindrical coordinates such as $\mathbf{r} = \rho\hat{\boldsymbol{\rho}} + z\hat{\boldsymbol{z}}$ with $\hat{\boldsymbol{\rho}} \cdot \hat{\boldsymbol{z}} = 0$, the Fourier transformation of the electron-ion interaction potential in collisional Lorentzian plasmas is obtained as follows:

$$\tilde{V}(\bar{q}) = -4\pi Z e^2 a_Z^2 \int_0^\infty d\bar{\rho}\,\bar{\rho} \int_0^\infty d\bar{z} \left[\frac{1}{(\bar{\rho}^2+\bar{z}^2)^{1/2}} e^{-(\bar{\rho}^2+\bar{z}^2)^{1/2}/\bar{\lambda}_\kappa} \cos(\bar{q}\,\bar{z}) \right.$$

$$+ \frac{2\sqrt{2}}{\sqrt{\pi}} \bar{\lambda}_\kappa^2 \left(\frac{v_0}{v_T} \right) \frac{1}{\mu_\kappa} \frac{\bar{z}}{(\bar{\rho}^2+\bar{z}^2)^2} (-i) \sin(\bar{q}\,\bar{z}) \qquad (7)$$

$$\left. + \left(2 - \frac{7\pi}{12} \right) \bar{\lambda}_\kappa^2 \left(\frac{\bar{\nu} v_0}{v_T} \right) \frac{1}{\mu_\kappa^2} \frac{\bar{z}}{(\bar{\rho}^2+\bar{z}^2)^{3/2}} (-i) \sin(\bar{q}\,\bar{z}) \right]$$

$$= -4\pi Z e^2 \bar{\lambda}_\kappa^2 a_Z^2 \tilde{\bar{V}}(\bar{q}),$$

where $\bar{q}(\equiv q/a_Z)$ is the scaled momentum transfer, $a_Z(=a_0/Z)$ is the Bohr radius of the hydrogenic ion with nuclear charge Ze, $a_0(=\hbar^2/me^2)$ is the Bohr radius of the hydrogen atom, $\bar{\lambda}_\kappa(\equiv\lambda_\kappa/a_Z)$ is the scaled effective Debye length, $\bar{\nu}(\equiv\nu a_Z/v_T)$ is the scaled collision frequency, and $\tilde{\bar{V}}(\bar{q})$ is the scaled Fourier transformation of the interaction potential:

$$\tilde{\bar{V}}(\bar{q}) = \frac{1}{1+(\bar{q}\bar{\lambda}_\kappa)^2} - i \left[\sqrt{\frac{\pi}{2}} \left(\frac{v_0}{v_T} \right) \frac{1}{\mu_\kappa} + \left(2 - \frac{7\pi}{12} \right) \left(\frac{\bar{\nu} v_0}{v_T} \right) \frac{1}{\mu_\kappa^2} \frac{1}{\bar{q}} \right]. \qquad (8)$$

where the first term in the right-hand-side represents the Fourier transform of the Debye potential. Then, the bremsstrahlung cross section can be rewritten in the following form:

$$d^2\sigma_b = \frac{16}{3} \frac{\alpha^3 a_Z^2}{\bar{E}} Z^2 \bar{\lambda}_\kappa^2 \left| \tilde{\bar{V}}(\bar{q}) \right|^2 \bar{q}^3\, d\bar{q} \frac{d\omega}{\omega}, \qquad (9)$$

where $\bar{E}(\equiv mv_0^2/2Z^2Ry)$ is the scaled energy of the projectile electron and $Ry(=me^4/2\hbar^2 \approx 13.6\,\mathrm{eV})$ is the Rydberg constant. It has been known that the bremsstrahlung emission spectrum would be investigated through the bremsstrahlung

radiation cross section [14] defined as $d^2\chi_b / d\bar{\varepsilon} d\bar{q} \equiv (d^2\sigma_b / \hbar d\omega d\bar{q})\hbar\omega$, where $\bar{\varepsilon} \equiv (\hbar\omega / Z^2 Ry)$ is the scaled radiation photon energy. After some mathematical manipulations, the bremsstrahlung radiation cross section $d\chi_b / d\bar{\varepsilon}$ due to the electron-ion interaction in warm collisional Lorentzian plasmas is obtained as followings:

$$\begin{aligned}\frac{d\chi_b}{d\bar{\varepsilon}} &= \frac{16}{3}\frac{\alpha^3 a_Z^2}{\bar{E}} Z^2 \bar{\lambda}_\kappa^4 \int_{\bar{q}_{\min}}^{\bar{q}_{\max}} d\bar{q}\, \bar{q}^3 \left|\tilde{\bar{V}}(\bar{q})\right|^2 \\ &= \frac{16}{3}\frac{\alpha^3 a_Z^2}{\bar{E}} Z^2 \bar{\lambda}_\kappa^4 \int_{\bar{q}_{\min}}^{\bar{q}_{\max}} d\bar{q}\, \bar{q}^3 \left\{ \left[\frac{1}{1+(\bar{q}\bar{\lambda}_\kappa)^2} \right]^2 \right. \\ &\qquad \left. + \left[\sqrt{\frac{\pi}{2}} \left(\frac{v_0}{v_T} \right) \frac{1}{\mu_\kappa} + \left(2 - \frac{7\pi}{12} \right) \left(\frac{\bar{\nu} v_0}{v_T} \right) \frac{1}{\mu_\kappa^2} \frac{1}{\bar{q}} \right]^2 \right\},\end{aligned} \tag{10}$$

where $\bar{q}_{\min}[\equiv (k_0 - k_f)a_Z] = \sqrt{\bar{E}/2} - \sqrt{(\bar{E} - \bar{\varepsilon})/2}$ is the scaled minimum momentum transfer and $\bar{q}_{\max}[\equiv (k_0 + k_f)a_Z] = \sqrt{\bar{E}/2} + \sqrt{(\bar{E} - \bar{\varepsilon})/2}$ is the scaled maximum momentum transfer. The electron-ion bremsstrahlung radiation cross section $d\chi_b / d\bar{\varepsilon}$ in units of πa_0^2 including the electron-electron collision effects is then found to be

$$\begin{aligned}\frac{d\chi_b}{d\bar{\varepsilon}} / \pi a_0^2 &= \frac{16}{3\pi}\frac{\alpha^3}{\bar{E}} \left\{ \left[\frac{1}{1+(\bar{q}_{\max}\bar{\lambda}_\kappa)^2} - \frac{1}{1+(\bar{q}_{\min}\bar{\lambda}_\kappa)^2} \right] + \ln\left[\frac{1+(\bar{q}_{\max}\bar{\lambda}_\kappa)^2}{1+(\bar{q}_{\min}\bar{\lambda}_\kappa)^2} \right] \right. \\ &\quad + \bar{\lambda}_\kappa^4 \left[\frac{\pi}{2} \left(\frac{\bar{E}}{\bar{E}_T} \right) \frac{1}{\mu_\kappa^2} \left(\bar{q}_{\max}^4 - \bar{q}_{\max}^4 \right) \right. \\ &\quad + \frac{8}{3}\sqrt{\frac{\pi}{2}} \left(2 - \frac{7\pi}{12} \right) \left(\frac{\bar{E}}{\bar{E}_T} \right) \frac{\bar{\nu}}{\mu_\kappa^3} \left(\bar{q}_{\max}^3 - \bar{q}_{\max}^3 \right) \\ &\quad \left. \left. + 2\left(2 - \frac{7\pi}{12} \right)^2 \left(\frac{\bar{E}}{\bar{E}_T} \right) \frac{\bar{\nu}^2}{\mu_\kappa^4} \left(\bar{q}_{\max}^2 - \bar{q}_{\max}^2 \right) \right] \right\},\end{aligned} \tag{11}$$

where $\bar{E}_T \equiv E_T / Z^2 Ry$. If we neglect the electron-electron collision effects in Lorentzian plasmas, i.e., the case of the ordinary Debye-Hückel potential with the effective Debye length $\bar{\lambda}_\kappa$, the electron-ion bremsstrahlung radiation cross section $d\chi_b' / d\bar{\varepsilon}$ becomes

$$\frac{d\chi_b'}{d\bar{\varepsilon}} / \pi a_0^2 = \frac{16}{3\pi}\frac{\alpha^3}{\bar{E}}\left\{\left[\frac{1}{1+(\bar{q}_{\max}\bar{\lambda}_\kappa)^2} - \frac{1}{1+(\bar{q}_{\min}\bar{\lambda}_\kappa)^2}\right] + \ln\left[\frac{1+(\bar{q}_{\max}\bar{\lambda}_\kappa)^2}{1+(\bar{q}_{\min}\bar{\lambda}_\kappa)^2}\right]\right\}. \quad (12)$$

In order to investigate the effects of electron-electron collisions and non-Maxwellian character on the electron-ion bremsstrahlung process in Lorentzian plasmas, we set $\bar{E} < \bar{E}_T$ since the interaction potential [Eq. (6)] would be valid for $v_0 < v_\kappa$. Figure 1 shows that the scaled bremsstrahlung radiation cross section $\partial_{\bar{\varepsilon}}\bar{\chi}_b [\equiv (d\chi_b / d\bar{\varepsilon}) / \pi a_0^2]$ as a function of the scaled photon energy $\bar{\varepsilon}$ and spectral index κ. As it is seen, the bremsstrahlung radiation cross section decreases with an increase of the radiation photon energy. It is also shown that the bremsstrahlung radiation cross section increases with increasing the spectral index. Hence, we found that the non-Maxwellian character of the Lorentzian plasma suppresses the bremsstrahlung emission spectrum. Figures 2 and 3 represent the bremsstrahlung radiation cross sections $\partial_{\bar{\varepsilon}}\bar{\chi}_b$ as functions of the radiation photon energy $\bar{\varepsilon}$ for various values of the electron-electron collision frequency $\bar{\nu}$ for small and large values of the spectral index, respectively. From these figures, we found that the electron-electron collision effects enhance the bremsstrahlung emission spectrum. It is also found that the collision effects slightly decrease with increasing the radiation photon energy. Figure 4 represents the three-dimensional plot of the bremsstrahlung radiation cross section $\partial_{\bar{\varepsilon}}\bar{\chi}_b$ as a function of the scaled collision frequency $\bar{\nu}$ and spectral index κ. The electron-electron collision effects on the bremsstrahlung radiation cross section are found to be more significant for large values of the spectral index. Thus, it is expected that the collision effects are more significant in Maxwellian plasmas. In addition, Figure 5 shows the

bremsstrahlung radiation cross section $\partial_{\bar{\varepsilon}}\overline{\chi}_b$ as a function of the spectral index κ for various values of $\overline{E}_T$. As shown, the bremsstrahlung radiation cross section increases with an increase of $\overline{E}_T$. In addition, the temperature effects are also found to be more significant for large values of the spectral index. Hence, it can be also expected that the electron-ion interactions in Maxwellian plasmas including electron-electron collisions produce stronger bremsstrahlung emission spectra than those in Lorentzian plasmas. From this work, we have found that the effects of electron-electron collisions and non-Maxwellian character play significant roles in the bremsstrahlung emission spectrum due to the electron-ion interactions in Lorentzian plasmas. These results would provide useful information on the bremsstrahlung emission spectrum in warm collisional thermal and non-thermal plasmas.

Acknowledgments

One of the authors (Y.-D. Jung) gratefully acknowledges the Director-General Professor O. Motojima, Director Professor M. Sato, Director Professor Y. Hirooka, and Professor I. Murakami for warm hospitality while visiting the National Institute for Fusion Science (NIFS) in Japan as a long-term visiting professor. He also thanks to Hanyang University for granting him a year-long sabbatical leave.

This work was supported by the Korea Research Foundation Grant funded by the Korean Government (MOEHRD, Basic Research Promotion Fund) (KRF-2007-313-C00169).

References

[1] Bethe H A and Salpeter E E 1957 *Quantum Mechanics of One- and Two-Electron Atoms* (Berlin: Springer-Verlag)

[2] Bekefi G 1966 *Radiation Processes in Plasmas* (New York: Wiley)

[3] Gould R J 1900 *Astrophys. J.* **362**, 284

[4] Jung Y-D and Jeong H-D 1996 *Phys. Rev. E* **54** 1912

[5] Shevelko V P 1997 *Atomic and Their Spectroscopic Properties* (Berlin: Springer-Verlag)

[6] Smirnov M 2000 *Clusters and Small Particles in Gases and Plasmas* (New York: Springer-Verlag)

[7] Beyer H F and Shevelko V P 2003 *Introduction to the Physics of Highly Charged Ions* (Bristol: Institute of Physics)

[8] Hasegawa A, Mima K and Duong-Van M 1985 *Phys. Rev. Lett.* **54** 2608

[9] Meng Z, Thorne R M and Summers D,1992 *J. Plasma Phys.* **47** 445

[10] Rubab N and Murtaza G 2006 *Phys. Scr.* **73** 178

[11] Stenflo L and Yu M Y 1973 *Phys. Scr.* **8** 301

[12] Yu M Y, Tegeback R and Stenflo L 1973 *Z. Phys.* **264** 341

[13] Bhatnagar P L, Gross E P and Krook M 1954 Phys. Rev. 94 511

[14] Jackson J D 1999 Classical Electrodynamics, 3rd ed. (New York: Wiley)

Figure Captions

Figure 1. The three-dimensional plot of the scaled bremsstrahlung radiation cross section $\partial_{\bar{\varepsilon}}\bar{\chi}_b$ as a function of the scaled photon energy $\bar{\varepsilon}$ and spectral index κ for $\bar{\lambda}_D = 50$, $\bar{E} = 10$, $\bar{E}_T = 20$, and $\bar{\nu} = 1$.

Figure 2. The scaled bremsstrahlung radiation cross section $\partial_{\bar{\varepsilon}}\bar{\chi}_b$ as a function of the scaled photon energy $\bar{\varepsilon}$ for $\kappa = 2$, $\bar{\lambda}_D = 50$, $\bar{E} = 20$, and $\bar{E}_T = 30$. The solid line represents the result for $\bar{\nu} = 0$, the dashed line for $\bar{\nu} = 1$, and the dotted line for $\bar{\nu} = 2$.

Figure 3. The scaled bremsstrahlung radiation cross section $\partial_{\bar{\varepsilon}}\bar{\chi}_b$ as a function of the scaled photon energy $\bar{\varepsilon}$ for $\kappa = 9$. The conditions are the same as in Figure 2.

Figure 4. The three-dimensional plot of the scaled bremsstrahlung radiation cross section $\partial_{\bar{\varepsilon}}\bar{\chi}_b$ as a function of the scaled electron-electron collision frequency $\bar{\nu}$ and spectral index κ for $\bar{\lambda}_D = 50$, $\bar{E} = 20$, $\bar{\varepsilon} = 10$, and $\bar{E}_T = 30$.

Figure 5. The scaled bremsstrahlung radiation cross section $\partial_{\bar{\varepsilon}}\bar{\chi}_b$ as a function of the spectral index κ for $\bar{\lambda}_D = 50$, $\bar{E} = 20$, $\bar{\varepsilon} = 10$, and $\bar{\nu} = 1$. The solid line represents the result for $\bar{E}_T = 30$, the dashed line for $\bar{E}_T = 40$, and the dotted line for $\bar{E}_T = 50$.

Figure 1

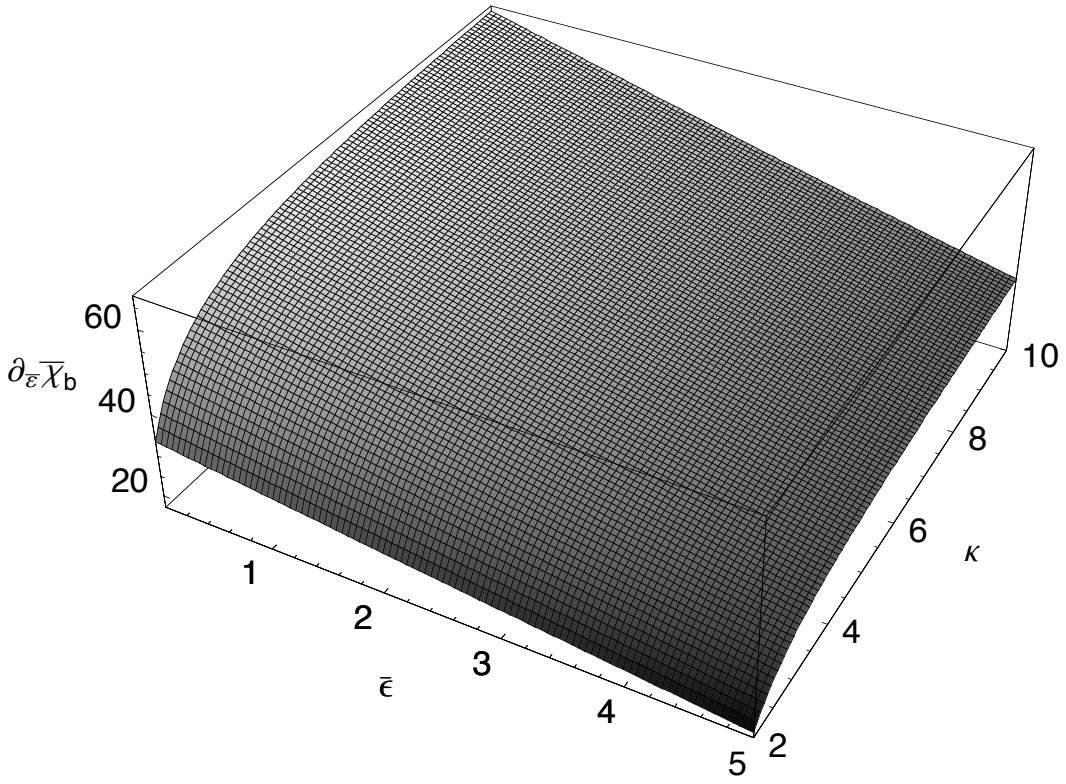
$\partial_{\bar{\varepsilon}}\overline{\chi}_{\mathrm{b}}$
60
40
20
1
2
3
4
5
$\bar{\epsilon}$
2
4
6
8
10
κ

Figure 2

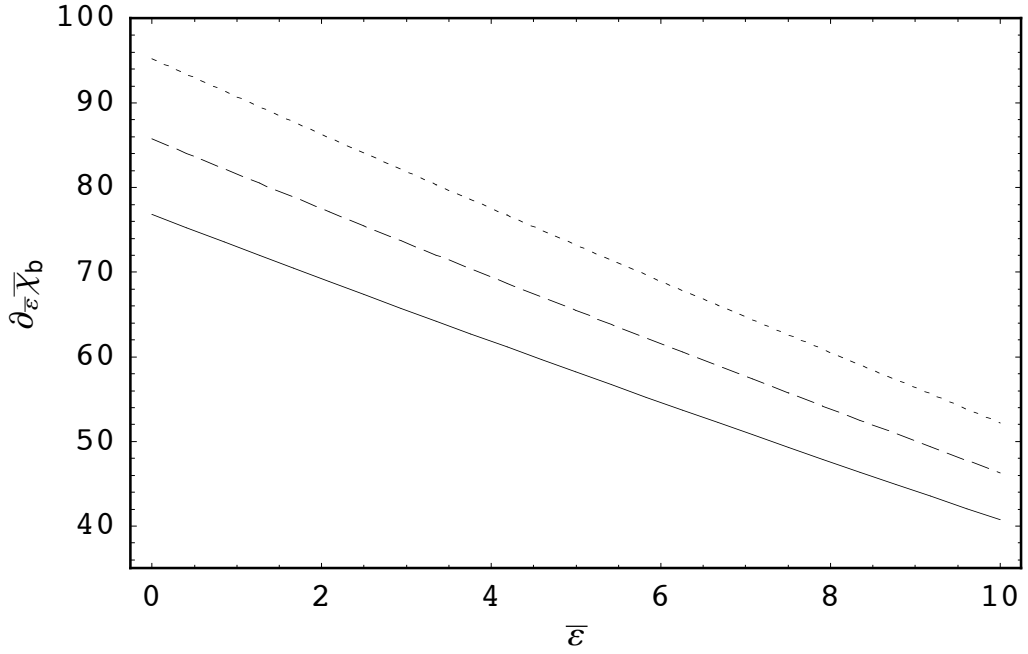
100
90
80
70
60
50
40
0
2
4
6
8
10
$\partial_{\overline{\varepsilon}}\overline{\chi}_b$
$\overline{\varepsilon}$

Figure 3

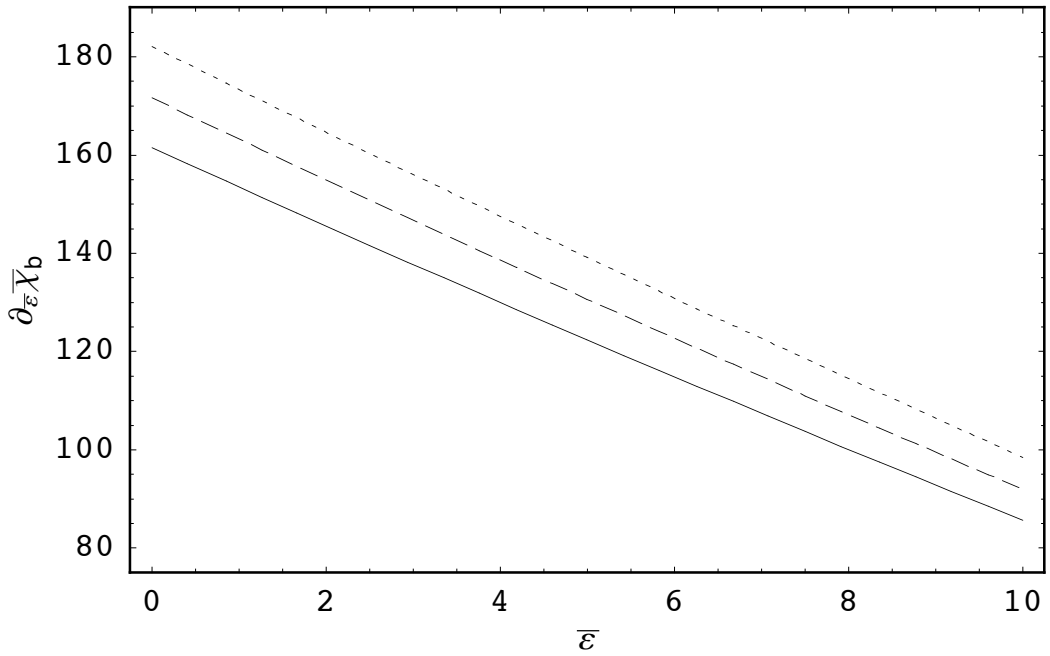
180
160
140
120
100
80
0
2
4
6
8
10
$\partial_{\overline{\varepsilon}}\overline{\chi}_b$
$\overline{\varepsilon}$

Figure 4

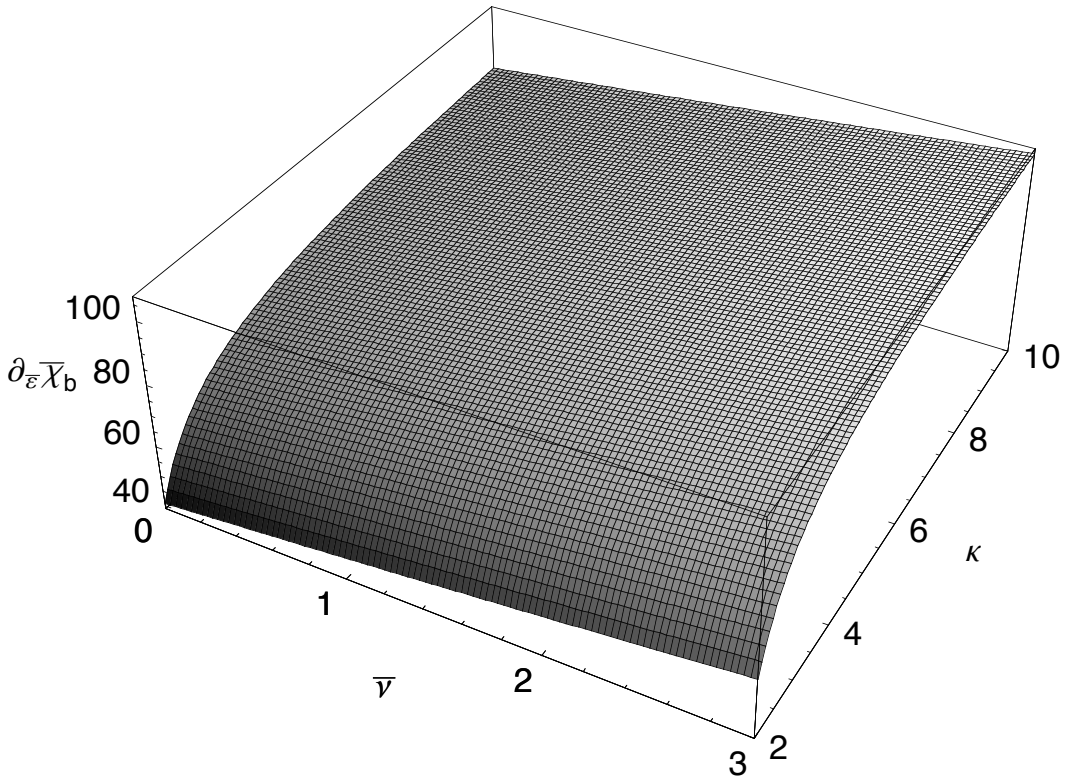
100
$\partial_{\overline{\varepsilon}}\overline{\chi}_b$ 80
60
40
0
1
$\overline{v}$
2
3
2
4
6
8
10
κ

Figure 5

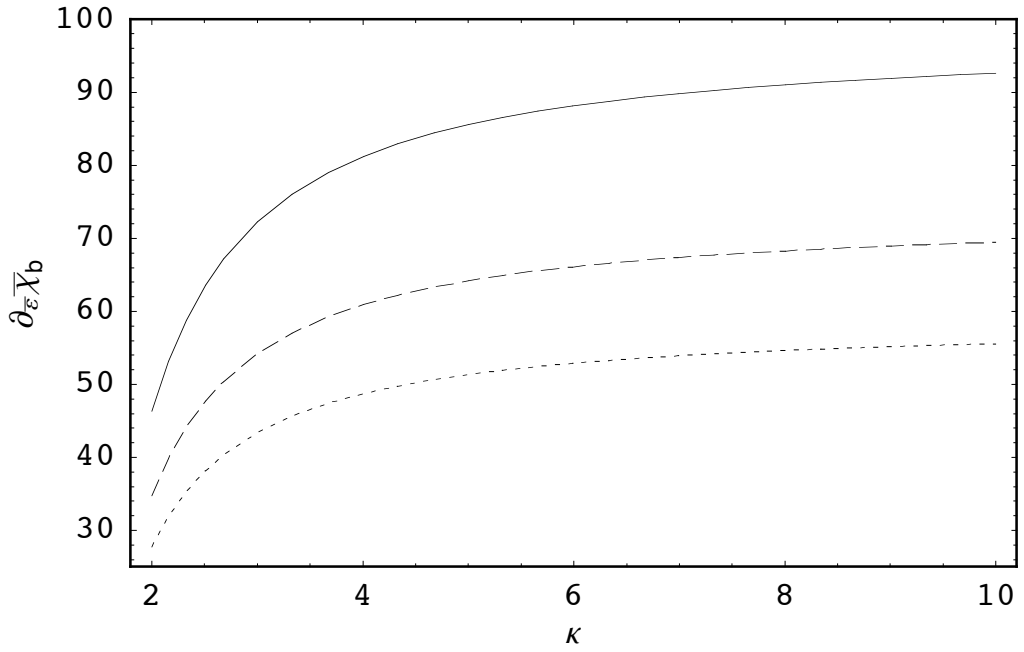
100
90
80
70
60
50
40
30
2
4
6
8
10
$\partial_\varepsilon \overline{\chi}_b$
κ